

The bias-controlled giant magnetoimpedance effect caused by the interface states in a metal-insulator-semiconductor structure with the Schottky barrier

Cite as: Appl. Phys. Lett. **104**, 222406 (2014); <https://doi.org/10.1063/1.4881715>

Submitted: 24 April 2014 . Accepted: 23 May 2014 . Published Online: 04 June 2014

N. V. Volkov, A. S. Tarasov, D. A. Smolyakov, A. O. Gustaitsev, V. V. Balashev, and V. V. Korobtsov



View Online



Export Citation



CrossMark

ARTICLES YOU MAY BE INTERESTED IN

[Extremely high magnetic-field sensitivity of charge transport in the Mn/SiO₂/p-Si hybrid structure](#)

AIP Advances **7**, 015206 (2017); <https://doi.org/10.1063/1.4974876>

[Frequency-dependent magnetotransport phenomena in a hybrid Fe/SiO₂/p-Si structure](#)

Journal of Applied Physics **112**, 123906 (2012); <https://doi.org/10.1063/1.4769788>

[Extremely large magnetoresistance induced by optical irradiation in the Fe/SiO₂/p-Si hybrid structure with Schottky barrier](#)

Journal of Applied Physics **114**, 093903 (2013); <https://doi.org/10.1063/1.4819975>

Meet the Next Generation
of Quantum Analyzers

And Join the Launch
Event on November 17th



Register now



Zurich
Instruments

The bias-controlled giant magnetoimpedance effect caused by the interface states in a metal-insulator-semiconductor structure with the Schottky barrier

N. V. Volkov,^{1,2,a)} A. S. Tarasov,¹ D. A. Smolyakov,¹ A. O. Gustaitsev,^{1,2} V. V. Balashev,^{3,4} and V. V. Korobtsov^{3,4}

¹Kirensky Institute of Physics, Russian Academy of Sciences, Siberian Branch, Krasnoyarsk 660036, Russia

²Institute of Engineering Physics and Radio Electronics, Siberian Federal University, Krasnoyarsk 660041, Russia

³Institute of Automation and Control Processes, Russian Academy of Sciences, Far East Branch, Vladivostok 690041, Russia

⁴School of Natural Sciences, Far Eastern Federal University, Vladivostok 690950, Russia

(Received 24 April 2014; accepted 23 May 2014; published online 4 June 2014)

We demonstrate that *ferromagnetic metal/insulator/semiconductor* hybrid structures represent a class of materials with the giant magnetoimpedance effect. In a metal-insulator-semiconductor diode with the Schottky barrier fabricated on the basis of the Fe/SiO₂/n-Si structure, a drastic change in the impedance in an applied magnetic field was found. The maximum value of this effect was observed at temperatures of 10–30 K in the frequency range of 10 Hz–1 MHz where the ac magnetoresistance and magnetoreactance ratios exceeded 300% and 600%, respectively. In the low-frequency region (<1 kHz), these ratios could be controlled in wide range by applying bias to the device. The main contribution to the impedance when measured at temperatures corresponding to the strongest magnetic-field sensitivity comes from the interface states localized near the SiO₂/n-Si interface and the processes of their recharging in an applied ac voltage. The applied magnetic field changes the energy structure of the interface states, thus affecting the processes of the charging dynamics. © 2014 AIP Publishing LLC. [<http://dx.doi.org/10.1063/1.4881715>]

The search for the systems with the giant magnetoimpedance (GMI) has been of great importance due to their high potential for applications in magnetic sensors and devices.^{1,2} First, the attention of researchers was focused mainly on nanocrystalline soft magnetic ribbons and films that exhibited a significant GMI ratio.³ In these materials, the GMI effect is due to the dependence of the impedance on skin depth and, consequently, ac transverse permeability, which, in turn, can be sensitive to a magnetic field.⁴ Such mechanism suggests that large value of the magnetoimpedance can be observed only at high-frequency (>10 MHz) currents, when the skin effect is predominant.⁵ When those studies were extended to multilayers, it was found that the structures with two soft magnetic layers sandwiching a highly conductive metal could have significant GMI ratio even without the onset of strong skin effect, i.e., at relatively low frequencies (<10 MHz).⁶ The main contribution to the impedance of the sandwiched films was found due to an inductive component, which significantly changed in magnetic field.⁷ Authors believe that the redistribution of the ac current density across the film thickness could be account for the observed phenomenon.

It is obvious that the high-frequency GMI effect can also be revealed in magnetic materials and structures with the dc giant magnetoresistance (GMR).⁸ It should be taken into account, however, that the ac magnetotransport will be additionally affected by magnetic permeability, microstructure, topology, and composition of multilayer structures and materials. For example, in the magnetic tunnel junction with MgO barriers, the ac tunneling magnetoresistance was consistent with its dc value, but the magnetocapacitance was

found to be larger than expected should one do the extraction based on the junction geometry only.⁹ In a tunnel structure with the Al₂O₃ barrier, a huge (over ±17 000%) change in the imaginary part of the impedance between the magnetically parallel and antiparallel states of the junction was found, although the dc GMR ratio was 15%.¹⁰ To date, there has been no unified explanation of the GMI effect in the tunnel junctions, although it seems related to the interplay of the spin dynamics and dielectric relaxation,¹¹ as well as the screening caused by charge and spin accumulation at the interfaces.¹⁰

In this work, we present a class of the magnetic systems with the GMI effect caused by a mechanism that has not been discussed before. These are the *ferromagnetic metal (FM)/insulator/semiconductor* hybrid structures with the interface states localized near the *insulator/semiconductor* interface, which energy structure is sensitive to an external magnetic field.

The sample to investigate was a metal-insulator-semiconductor (MIS) diode with the Schottky barrier fabricated in the Fe/SiO₂/n-Si hybrid structure. To prepare the Fe/SiO₂/n-Si structure, we used an n-Si(100) wafer with a resistivity of 7.5 Ω·cm (a doping density of 10¹⁵ cm⁻³). The substrate's surface was pre-cleaned by Shiraki method.¹² SiO₂ layer with the thickness of 1.5 nm was formed on the substrate's surface using a chemical method.¹³ Then, 10 nm thick iron film was deposited by thermal evaporation.

Impedance spectra of the MIS diode were studied using the two-probe configuration. The device and measuring setup are schematically illustrated in the inset of Fig. 1(a). One probe was attached to the Fe electrode top by silver epoxy; the other probe, to the substrate backside via Al-Ga contact.

^{a)}E-mail: volk@iph.krasn.ru

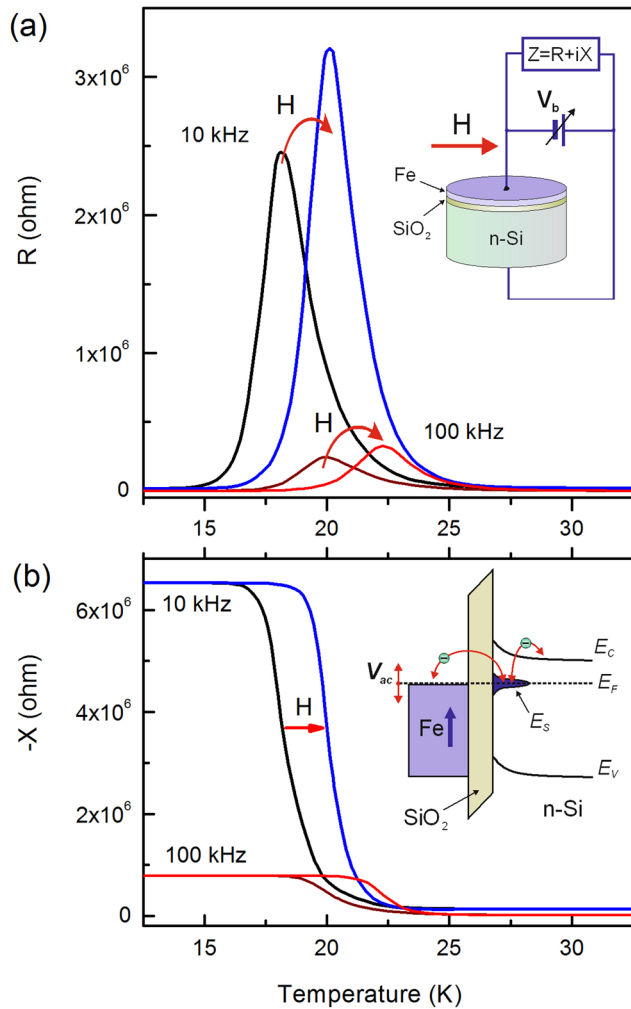


FIG. 1. Temperature dependences of (a) the real and (b) imaginary parts of the impedance at 10 and 100 kHz in zero and 1 T magnetic field. Insets: (a) schematic of the device and measuring setup and (b) schematic band diagram of the Fe/SiO₂/n-Si Schottky diode with the interface levels.

The real (R) and imaginary (X) parts of the impedance $Z = R + iX$ were measured by an Agilent E4980A analyzer in the frequency range from 20 Hz to 2 MHz. The measuring setup allowed the dc bias voltage up to ± 5 V to be applied across the device.

The strong effect of the magnetic field on the impedance of the device was observed in relatively narrow temperature range of 10–30 K, where there was an intense peak in the temperature dependence of the real part of impedance ($R(T)$) and the corresponding step in the behavior of the imaginary component ($X(T)$). It can be seen in Fig. 1 that the magnetic field effect manifests itself as a shift of the $R(T)$ peak and the corresponding $X(T)$ step at higher temperatures. For the magnetic field of 1 T, this shift is about 2 K. The variation in the $R(T)$ in the magnetic field gives us a hint for possible cause of the unusual behavior of the real part of the impedance at this particular fixed temperature (Fig. 2(a)). The $R(H)$ shape depends on the $R(T)$ peak portion at which the system is located at $H = 0$. This position is completely determined by the temperature. Figure 2(a) demonstrates that by choosing proper temperature, it is possible to see either positive or negative magnetoresistance or even the change in the magnetoresistive effect sign at certain H . Here, we define the

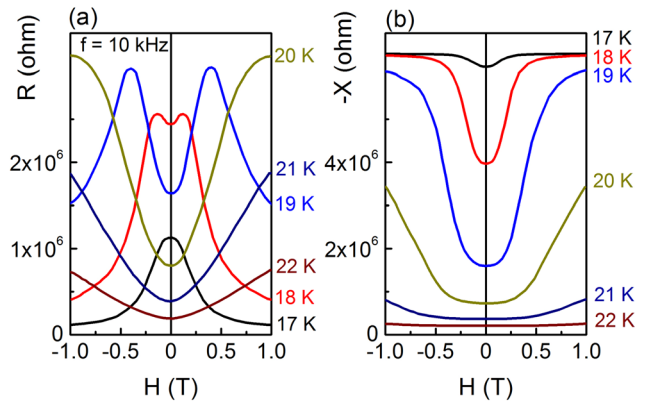


FIG. 2. (a) Real and (b) imaginary parts of the impedance vs magnetic field dependence at different temperatures ($f = 10$ kHz).

magnetoresistance as $MR = 100\% \times \frac{R(H) - R(0)}{R(0)}$. The effect of H on the reactance ($X(H)$) was simpler (Fig. 2(b)): since the magnetic field caused the $X(T)$ step shift to higher temperatures, only the positive magnetoreactance is realized ($MX = 100\% \times \frac{X(H) - X(0)}{X(0)}$). Both MX value and $X(H)$ dependence were temperature-dependent.

Since the magnetic field effect is not observed beyond the discussed features, we guess it is reasonable to attribute the field sensitivity of the ac transport properties of the MIS diode to the processes responsible for the occurrence of these features in $R(T)$ and $X(T)$. In the MIS structures, the $R(T)$ peaks and corresponding $X(T)$ steps were caused solely by a delay in recharging of the interface states localized near the insulator/semiconductor interface.¹⁴ Those recharging processes may be affected by the ac-measurements since as the voltage V_{ac} was applied to the MIS structure it swept the Fermi level through the interface center energy levels (inset in Fig. 1(b)). The $R(T)$ peak should occur under the condition $\omega \langle \tau \rangle = 1$, where $\omega = 2\pi f$ is the angular frequency of V_{ac} and $\langle \tau \rangle$ is the average relaxation time that characterizes the charge-discharge process at or near the interface. In general, the relaxation time is $\tau = \tau_0 \exp\left(\frac{E_s}{k_B T}\right)$, where E_s is the energy of the interface state relative to the bottom of the conduction band (E_C) and τ_0 is the prefactor determined by a number of parameters. For an ideal MIS structure, the interface states charge-discharge processes are due to the capture-emission of electrons from the interface states to the conduction band. Here, prefactor τ_0 is determined by the electron capture cross-section, density of states in the conduction band, and degeneracy factor of the interface states. For the MIS structure under study, the SiO₂ potential barrier width was about 1 nm; therefore, it is necessary to take into account electron tunneling between the interface levels and the metal electrode through the potential barrier. Therefore, we believe that the interface states would recharge via sequential process, which had both the electron capture-emission, and electron tunneling from the metal electrode to the interface states and backwards. As a result, τ_0 depended upon the tunneling probability and the density of states in the metal electrode.

The character of the features in the temperature dependence of the impedance suggests that the $R(T)$ peak and $X(T)$ step positions are frequency-dependent. With increasing ω ,

the features should shift to higher temperatures. It is this behavior that is observed in our measurements both at $H = 0$ and in nonzero magnetic fields. As an example, Fig. 1 shows the $R(T)$ and $X(T)$ dependences obtained at frequencies of 10 and 100 kHz.

The observed rapid reduction of the $R(T)$ peak height and the $X(T)$ step amplitude with increasing frequency of the applied ac-voltage might be related to the semiconductor in-gap behavior of the interface states density function $N(E)$,¹⁴ namely: $N(E)$ has its maximum at $E = E_S$ and falls rapidly in the vicinity.

Thus, the shift of the $R(T)$ features in external magnetic field and, consequently, the GMI phenomenon in the MIS Fe/SiO₂/n-Si diode structure should apparently be considered in terms of the magnetic field effect on the energy spectrum of the localized states at or near the SiO₂/n-Si interface. We may conclude that in the applied field, E_S shifts towards E_C and the form of $N(E)$ also slightly changes. Indeed, in this case, the Fermi level shifts toward E_C in the n-type semiconductor as the temperature is decreased, therefore it crosses the energy levels of the interface states at higher temperatures than it would do without field. Therefore, the $R(T)$ peak and $X(T)$ step in the field are also observed at higher temperatures. We believe that the variation of $N(E)$ manifests itself in the growth of the $R(T)$ peak height and the change of its shape.

Positions of the energy levels of the surface states in the band gap and E_S in magnetic field can be roughly estimated with the use of the simple relation $\ln(\omega) = \ln\left(\frac{1}{\tau_0} - \frac{E_S}{k_B T_p}\right)$, where T_p is the $R(T)$ peak position at fixed ω . For simplicity, we assume τ_0 to be independent of T . Fitting the experimental $\ln(\omega)$ dependence by a straight line, we estimated E_S from the line slope; the intercept gives the value of τ_0 . Such a plot is shown in the inset in Fig. 3 for the data obtained at $H = 0$ and $H = 1$ T. Thus, obtained positions of E_S in zero and nonzero fields are 37.8 meV and 42.0 meV relative to

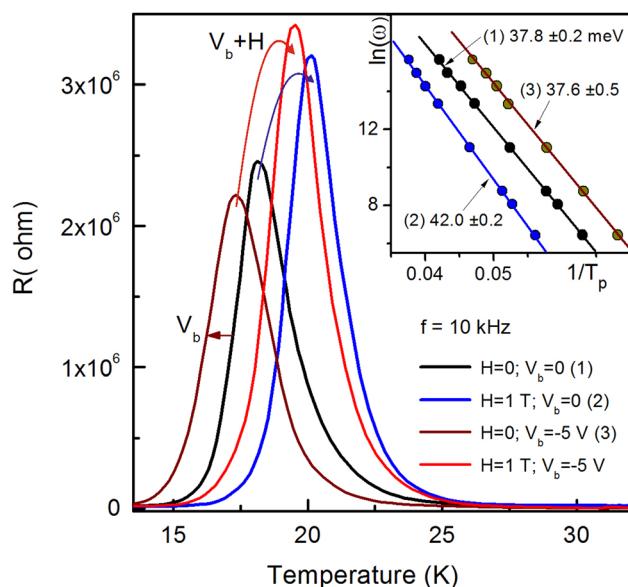


FIG. 3. Temperature dependences of the real part of the impedance ($f = 10$ kHz). Magnetic field shifts the peak toward higher temperatures, while reverse bias V_b shifts it in the opposite direction. Inset: $\ln(\omega)$ vs reciprocal peak temperature for determining energy levels, of the interface states.

E_C , respectively. The value of τ_0 remains nearly independent upon the magnetic field applied, which indicates that the field has very weak effect on parameters such as: capture coefficient, tunneling probability, and densities of states in the metal and semiconductor conduction band.

The shift of the energy levels of the surface states in magnetic field appeared surprisingly large: 4 meV. For comparison, the value of Zeeman splitting of the levels does not exceed 0.06 meV at $S = 1/2$ in a field of 1 T. Probably, such a large shift can be explained by the fact that the energy levels of the interface states split due to the exchange interaction with d-electrons in the ferromagnetic electrode near the interface¹⁵ or/and exchange interaction with the magnetic centers localized in SiO₂. Generally, the occurrence of ferromagnetic centers in SiO₂ is expected due to their diffusion from the 3d FM metals electrodes during the fabrication process of the FM/SiO₂/Si-based MIS structures.¹⁶ The same fact apparently explains another surprising result, specifically, the strong anisotropy of the magnetoimpedance. The effect of magnetic field oriented perpendicular to the structure plane appears much weaker than for the parallel orientation of the field. The shift of the $R(T)$ peak and corresponding $X(T)$ step is only ≈ 0.2 K in a field of 1 T. The final conclusion about the origin of such a behavior will be made after establishing the nature of the interface states and determining the mechanisms of the magnetic field effect on their energy structure. By now, these questions are unanswered.

It is well-known that by varying the bias V_b across the MIS structure, the position of the energy levels of the interface states changes according to the shift of the semiconductor band gap edges, whereas the position of the Fermi level remains invariable. Figure 3 shows that at the reverse bias $V_b < 0$, the $R(T)$ peaks and corresponding $X(T)$ steps shift toward lower temperatures by approximately the same values at $H = 0$ and $H = 1$ T. Analysis similar to that described above showed that at V_b up to -5 V, there was no noticeable variation of E_S (E_S was invariable within the measurement error), while τ_0 changed. At the same time, the behavior of the peak intensity indicates possible modification of $N(E)$. Positive bias ($V_b > 0$) up to -5 V did not noticeably affect the behavior of the $R(T)$ and $X(T)$ dependences. The latter is probably due to the fact that in the forward bias the potential main drop appears not across the MIS junction but across the semiconductor volume. In any case, given example demonstrates possibility of controlling the interface state related $R(T)$ and $X(T)$ features and, consequently, the values of MR and MX by changing the bias across the structure.

Information about the nature of the interface states and mechanisms of their recharging can be obtained from the frequency dependence of the real ($R(f)$) and imaginary ($X(f)$) parts of the impedance. Figures 4(a) and 4(b) present the $R(f)$ and $X(f)$ dependence at fixed temperature for $H = 0$ and $H = 1$ T, $V_b = 0$ and $V_b = -5$ V. Despite the limited data for full analysis of these dependences, we would like to qualitatively describe the main features in their behavior.

First, we consider the case $V_b = 0$. In the high-frequency range of 10^4 – 10^5 Hz, the investigated dependences are typical of the Debye relaxation processes: there are characteristic $R(f)$ steps and corresponding $X(f)$ peaks. We attribute this behavior to the inertial character of the interface state recharging

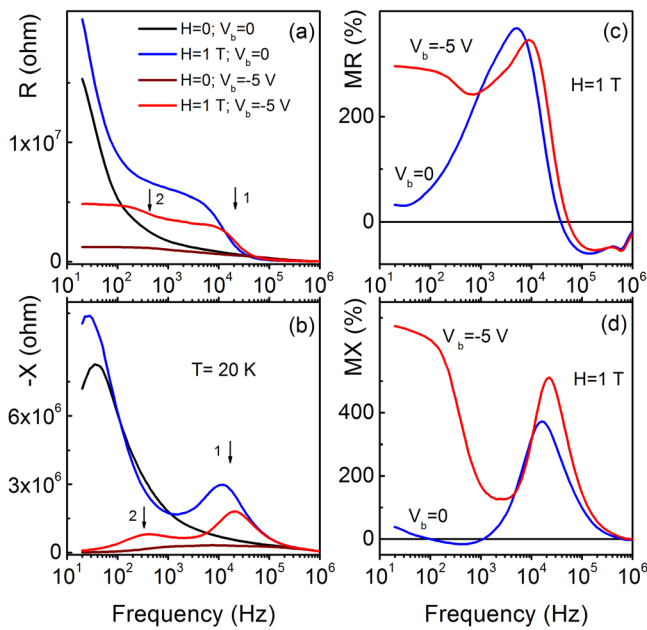


FIG. 4. (a) Real and (b) imaginary parts of the impedance vs frequency at $T = 20$ K. The dependences are recorded at zero bias and a reverse bias of -5 V in zero magnetic field and in a field of 1 T. Frequency dependences of (a) magnetoresistance and (b) magnetoreactance at zero bias and a bias of -5 V at T and K.

process, which occurs via the direct capture-emission involving the conduction band states. Frequency position of this feature, f_1 , is determined by the condition $f_1 = \frac{1}{2\pi\langle\tau\rangle}$; i.e., for the frequencies above f_1 the recharging process lags behind the variation in the ac voltage applied to the structure. It can be seen in Figs. 4(c) and 4(d) that the maximum values of MR and MX are observed just in the Debye anomaly region, i.e., the magnetic field sensitivity is maximum at the measuring current frequencies at which they coincide with the characteristic inverse relaxation time, which characterizes the interface state recharging delay. The rapid growth of R and $|X|$ with decreasing frequency is related not only to the surface centers but also to the slow generation-recombination processes that occur in the space charge region of the MIS structure.¹⁷ This is confirmed by the fact that such behavior was observed at temperatures where the interface-related features on $R(T)$ and $X(T)$ curves did not show up.

By applying the bias $V_b < 0$, one suppresses the growth of R and $|X|$ in the low-frequency region. The point is that when applying the negative bias an electron-depleted region forms near the interface of the MIS structure, which works as an additional insulator layer and reduces the total capacitance of the structure. At $V_b = -5$ V, one more Debye anomaly arises in the $R(T)$ and $X(T)$ dependences at the frequencies near $f_2 = 500$ Hz (Figs. 4(a) and 4(b)). We attribute this to the fact that at these frequencies, the interface states are recharged by a certain sequence of the capture-emission processes involving conduction band and electron tunneling through the potential barrier. Obviously, in this case, the relaxation time $\langle\tau\rangle$ should be larger than in the case of recharging solely by the direct capture-emission involving the conduction band.

Existence the depleted region at $V_b < 0$ indicates that near the tunnel junction, an additional electric field arises

that can affect the tunneling between the metal and the interface states. It is noteworthy that the occurrence of the Debye anomaly at low frequencies in an applied bias is accompanied by a significant increase of MR and MX just in the low-frequency region (Figs. 4(a) and 4(b)). In particular, MR increases approximately from 50% to 290% and MX , from 0% to 630% when varying the bias V_b from 0 to -5 V, at the frequency $f = 100$ Hz and magnetic field equal to $H = 1$ T. At higher frequencies, MR and MX do not change noticeably by the V_b bias. Thus, when analyzing possible mechanisms of the magnetic field effect on R and X , one should take into account, the field effect on the electron tunneling probability between the centers and the ferromagnetic electrode. The physical mechanism of this effect is yet to be figured out along with the cause of the increased sensitivity of interface centers energy structure to the magnetic field. From our point of view, one of the possible explanations could be formation of the impurity centers involving the Fe ions as they could diffuse through thin SiO_2 layer to appear at the $\text{SiO}_2/\text{n-Si}$ interface.¹⁷

Previously, we reported the unusual magnetotransport properties of simple devices based on the $\text{Fe}/\text{SiO}_2/\text{p-Si}$ hybrid structure on a p-type semiconductor substrate.^{18–20} We investigated the magnetoimpedance, but the value of the effect was much smaller. In addition, due to the features of the spectrum of the interface states at the $\text{SiO}_2/\text{p-Si}$ interface, we failed to explicitly separate and analyze the contribution of the magnetosensitive centers to the magnetoimpedance.

Thus, we demonstrated the giant magnetoimpedance effect in the hybrid $\text{Fe}/\text{SiO}_2/\text{n-Si}$ MIS structure. We showed that the effect is due to the presence of the interface states at the $\text{SiO}_2/\text{n-Si}$ interface, which participate in the recharging processes under the action of an ac-voltage applied to the structure. The magnetic field effect results mainly in shifting the interface state levels; however, at a certain dc bias, it is possible to modify the probability of electron tunneling through the potential barrier between the surface states and the ferromagnetic electrode. In our opinion, the hybrid structures in which the mechanism discussed here is observed can appear very promising for the creation of magnetic sensors and other microelectronic devices.

With the today's highly developed semiconductor technology, there are good opportunities to purposefully form the magnetic surface centers with a specified energy state in the semiconductor band gap of MIS structures and, thus, implement the magnetoimpedance sensors for operation in different temperature and, perhaps, frequency ranges.

This study was supported by the Russian Foundation for Basic Research, Project Nos. 14-02-00234-a and 14-02-31156; the Presidium of the Russian Academy of Sciences, program Quantum Mesoscopic and Disordered Structures, Project No. 20.8; and the Russian Ministry of Education and Science, Project No. 02.G25.31.0043.

¹R. S. Beach, N. Smith, C. L. Platt, F. Jeffers, and A. E. Berkowitz, *Appl. Phys. Lett.* **68**, 2753 (1996).

²M. H. Phan and H. X. Peng, *Prog. Mater. Sci.* **53**, 323 (2008).

³N. Laurita, A. Chaturvedi, C. Bauer, P. Jayatilaka, A. Leary, C. Miller, M.-H. Phan, M. E. McHenry, and H. Srikanth, *J. Appl. Phys.* **109**, 07C706 (2011).

- ⁴P. Ciureanu, L. G. C. Melo, D. Seddaoui, D. Menard, and A. Yelon, *J. Appl. Phys.* **102**, 073908 (2007).
- ⁵R. L. Sommera and C. L. Chienb, *Appl. Phys. Lett.* **67**, 3346 (1995).
- ⁶T. Morikawa, Y. Nishibe, H. Yamadera, Y. Nonomura, M. Takeuchi, and Y. Taga, *IEEE Trans. Magn.* **33**, 4367 (1997).
- ⁷K. Hika, L. V. Panina, and K. Mohri, *IEEE Trans. Magn.* **32**, 4594 (1996).
- ⁸J. Hu, H. Qin, B. Li, Y. Wang, and Y. Zhang, *J. Magn. Magn. Mater.* **323**, 1185 (2011).
- ⁹P. Padhan, P. LeClair, A. Gupta, K. Tsunekawa, and D. Diayaprawira, *Appl. Phys. Lett.* **90**, 142105 (2007).
- ¹⁰W. C. Chien, C. K. Lo, L. C. Hsieh, Y. D. Yao, X. F. Han, Z. M. Zeng, T. Y. Peng, and P. Lin, *Appl. Phys. Lett.* **89**, 202515 (2006).
- ¹¹M.-F. Kuo, C.-M. Fu, X.-F. Han, C.-O. Chang, and C.-S. Chou, *J. Appl. Phys.* **109**, 07C718 (2011).
- ¹²A. Ishizaka and Y. Shiraki, *J. Electrochem. Soc.* **133**, 666 (1986).
- ¹³T. Matsumoto, Y. Kubota, S. Imai, and H. Kobayashi, *ECS Trans.* **35**(4), 217–227 (2011).
- ¹⁴D. L. Losee, *J. Appl. Phys.* **46**, 2204 (1975).
- ¹⁵L. V. Lutsev, A. I. Stognij, and N. N. Novitskii, *Phys. Rev. B* **80**, 184423 (2009).
- ¹⁶M. Kanoun, R. Benabderrahmane, C. Duluard, C. Baraduc, N. Bruyant, A. Bsiesy, and H. Achard, *Appl. Phys. Lett.* **90**, 192508 (2007).
- ¹⁷S. M. Sze, *Semiconductor Devices* (Wiley, New York, 1985).
- ¹⁸N. V. Volkov, A. S. Tarasov, E. V. Eremin, S. N. Varnakov, S. G. Ovchinnikov, and S. M. Zharkov, *J. Appl. Phys.* **109**, 123924 (2011).
- ¹⁹N. V. Volkov, A. S. Tarasov, E. V. Eremin, A. V. Eremin, S. N. Varnakov, and S. G. Ovchinnikov, *J. Appl. Phys.* **112**, 123906 (2012).
- ²⁰N. V. Volkov, A. S. Tarasov, E. V. Eremin, F. A. Baron, S. N. Varnakov, and S. G. Ovchinnikov, *J. Appl. Phys.* **114**, 093903 (2013).